REPORT DOCUMENTATION PAGE

Form Approved
OBM No. 0704-0188

1. AGENCY USE ONLY *(Leave blank)*

2. REPORT DATE
14 December 1996

3. REPORT TYPE AND DATES COVERED
Contract Report

4. TITLE AND SUBTITLE
Adaptive Compression of Images

5. FUNDING NUMBERS
Job Order No.
Program Element No. 0603207N
Project No.
Task No.
Accession No.

6. AUTHOR(S)
George Zweig

7. PERFORMING ORGANIZATION NAME(S) AND ADDRESS(ES)
Signition, Incorporated, 417C Route 1, Espanola, NM 87532

8. PERFORMING ORGANIZATION REPORT NUMBER
NRL/CR/7241--97-0001

9. SPONSORING/MONITORING AGENCY NAME(S) AND ADDRESS(ES)
Naval Research Laboratory
Remote Sensing Branch
Stennis Space Center, MS 39529-5004

10. SPONSORING/MONITORING AGENCY REPORT NUMBER

11. SUPPLEMENTARY NOTES
In support of Basic Contract N00014-96-C-6007

12a. DISTRIBUTION/AVAILABILITY STATEMENT
Approved for public release; distribution is unlimited.

12b. DISTRIBUTION CODE

13. ABSTRACT *(Maximum 200 words)*

We propose an adaptive compression enhancement scheme for images, that faithfully preserves edges that exist at certain scales. The image gradient is decomposed in a wavelet basis to locate edges at specific scales. Based on their location, the corresponding wavelet coefficients in the wavelet decomposition of the image are earmarked for preservation. A scale-space localized implementation of the gradient operator is derived in the wavelet transform domain, based on the Lemarié-Rieusset diagonalization of the derivative operator for functions of one variable. By decomposing an image with respect to a standard biorthogonal wavelet basis, we succeed in obtaining the gradient (edge) information in the image (with respect to associated *hybrid* biorthogonal wavelet bases) at *certain desired scales only*. There are several advantages to and applications of such a localized implementation of the gradient, apart from its computational efficiency. Adaptive compression of images based on edge-strengths at specific scales becomes possible, so that compression can be less in the neighborhood of edges at those scales at which its characteristics are best represented. Such preferential compression capability is useful for the compression of vast databases of oceanographic and astronomical images; faint edges characterizing interfaces between warm and cold ocean currents in satellite oceanographic images, and boundaries between interstellar dust and nebulae of subtly varying luminosities in astronomical images are important image features that need to be preserved with minimum distortion, while achieving significant compression in other parts of these images that correspond to known features such as land-ocean boundaries or familiar stars.

14. SUBJECT TERMS
image compression, image gradients, wavelet coefficients, Lemarié-Rieusset diagonalization, ocean currents, satellite imagery, interstellar dust, nebulae, luminosities, and astronomical imagery

15. NUMBER OF PAGES
15

16. PRICE CODE

17. SECURITY CLASSIFICATION OF REPORT	18. SECURITY CLASSIFICATION OF THIS PAGE	19. SECURITY CLASSIFICATION OF ABSTRACT	20. LIMITATION OF ABSTRACT
Unclassified	Unclassified	Unclassified	SAR

Adaptive Compression of Images

George Zweig
Signition, Inc.
417C Route 1, Española, NM 87532
[redacted]

Progress Report 0001 prepared under contract for Ronald J. Holyer
— Code 7241, NRL-Stennis, Stennis Space Center, MS 39529-5004

December 14, 1996

Abstract

We propose an adaptive compression enhancement scheme for images, that faithfully preserves edges that exist at certain scales. The image gradient is decomposed in a wavelet basis to locate edges at specific scales. Based on their location, the corresponding wavelet coefficients in the wavelet decomposition of the image are earmarked for preservation . A scale-space localized implementation of the gradient operator is derived in the wavelet transform domain, based on the Lemarié-Rieusset diagonalization of the derivative operator for functions of one variable. By decomposing an image with respect to a standard biorthogonal wavelet basis, we succeed in obtaining the gradient (edge) information in the image (with respect to associated *hybrid* biorthogonal wavelet bases) at *certain desired scales only.* There are several advantages to and applications of such a localized implementation of the gradient, apart from its computational efficiency. Adaptive compression of images based on edge-strengths at specific scales becomes possible, so that compression can be less in the neighborhood of edges at those scales at which its characteristics are best represented. Such preferential compression capability is useful for the compression of vast databases of oceanographic and astronomical images; faint edges characterizing interfaces between warm and cold ocean currents in satellite oceanographic images, and boundaries between interstellar dust and nebulae of subtly varying luminosities in astronomical images are important image features that need to be preserved with minimum distortion, while achieving significant compression in other parts of these images that correspond to known features such as land-ocean boundaries or familiar stars.

1 Introduction

In many image processing applications it is necessary to partition an image into two subsets, where one of the subsets is a *distinguished subset* that contains points of the image at which a particular image characteristic or feature manifests itself. In this paper, we will be interested in extracting certain distinguished subsets of images, in order to selectively apply adaptive image compression . A distinguished subset may be obtained by means of an algorithm that processes the image for specific information, or an operator that acts on the image to enhance or suppress specific features. We will restrict ourselves here to a particular class of image processing operations, where the distinguished subset is obtained by means of a local operator; e.g., the derivative operator. By taking the wavelet transform of the result of such a local operator's action on an image, it is possible to separate the different positions and scales of the distinguished subset. Moreover, as a consequence of the locality of the operator, it is possible to effect changes in the neighborhoods of those coefficients in the wavelet transform of the image, that correspond in scale and space to the transform coefficients of the points of the distinguished subset. Furthermore, if the operator involved is linear, then it is possible to realize it entirely in the wavelet transform domain, allowing an efficient and localized implementation of it. Several local linear operators such as the gradient, the curl or rotation, the Laplacian and convolutions with compact kernels are important for extracting image features relevant to various image processing operations. In this paper we will develop wavelet based adaptive compression by means of the gradient operator.

2 Compression

Wavelet-based lossy compression of an image is achieved by expanding the image in an appropriate two-dimensional wavelet basis, and in each subband of the decomposition retaining only significant coefficients by means of a thresholding scheme. The thresholded decomposition of the image is subsequently quantized and encoded to achieve a lossy compressed image file. Existing lossy compression schemes are reasonably good at preserving flat regions of an image, where there are no sharp fluctuations in image intensity. They are, however, not well adapted to preserving certain image details such as edges and textures, which provide important visual cues and contribute to image quality. It is important therefore to preserve coefficients that lie in the neighborhoods of image features such as edges or textures, in order to obtain higher quality compressed images. In this paper we propose a method of locating and preserving image edge coefficients at desired scales using a wavelet-based implementation of the image gradient operator.

If $\mathcal{I}$ is an image, then the gradient of the image, $\nabla \mathcal{I} = \left(\frac{\partial \mathcal{I}}{\partial x}, \frac{\partial \mathcal{I}}{\partial y}\right)$, helps make edges in the image apparent. We will *use the small wavelet coefficients of the gradient $\nabla\mathcal{I}$ to selectively threshold the wavelet coefficients of the image $\mathcal{I}$, in order to compress it without disfiguring its edges.* Preserving wavelet coefficients in small neighborhoods of those wavelet coefficients corresponding to edges, will preserve the quality of the edges in the compressed image. Most important, it is possible to preserve edges at only certain desired scales and positions.

The wavelet decomposition of the gradient of an image expresses the scale-space structure of edges in the original image. The magnitudes of an edge's coefficients at any scale measure the strength of the edge at that scale, and their locations specify the location of the edge at that scale. This suggests that at any particular scale, preserving the neighborhoods of the edge coefficients of the image will preserve the edge features in the image at that scale. Identifying neighborhoods of edge coefficients in the wavelet decomposition of the gradient of an image at the desired scales, defines *edge masks*, which can be used to preserve coefficients of the image that correspond to edges at those scales.

The edge coefficients of the image at any scale correspond to *modulus maxima* (see Appendix B) of the image gradient's coefficients at that scale. However, the gradient of an image also accentuates transient image features other than edges, such as textures and noise. It is therefore necessary to distinguish between edge and non-edge coefficients at each scale of the wavelet decomposition of the image gradient. This distinction can be performed by means of the edge detection scheme outlined in Appendix B. The edge masks partition the image coefficient set at each scale into a distinguished subset consisting of the edge coefficients together with the coefficients contained in their 3×3-neighborhoods, and an undistinguished subset consisting of the remaining non-edge coefficients. An image coefficient is left unchanged, or only weakly thresholded, if it belongs to a distinguished subset, and is strongly thresholded otherwise. This scale-specific edge-adaptive compression scheme for images is summarized in the following diagram:

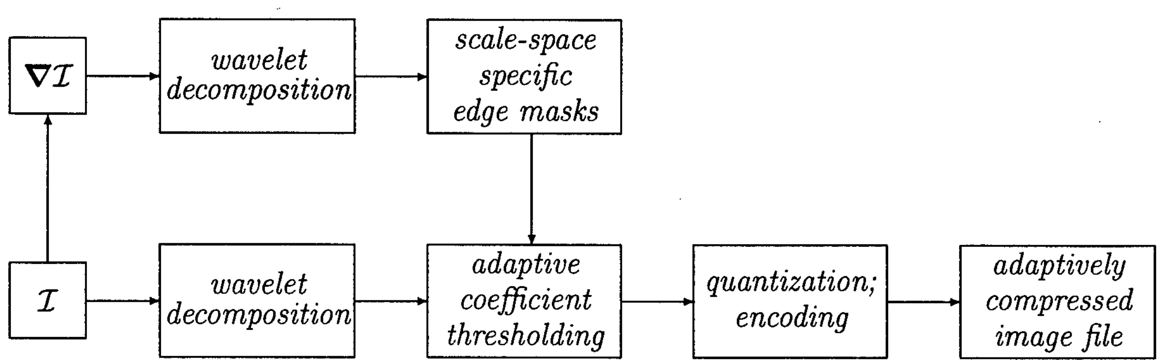

Fig. 1: Adaptive image compression scheme using image gradient information.

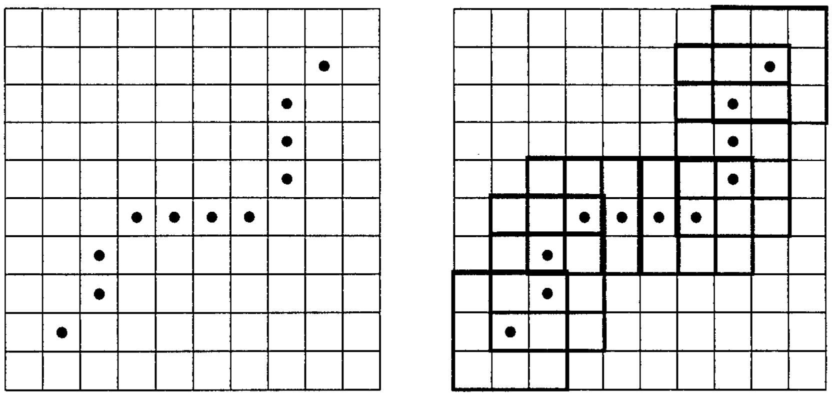

Fig. 2: Edge coefficients and their 3×3-neighborhoods

The above scheme is not restricted in its application to compression alone. In fact, it can be thought of as a paradigm for formulating and implementing scale-space specific local linear image processing operations in the wavelet transform domain. Indeed, it is easily adapted to enhancing edges in images, as described below.

3 Implementing the gradient in the wavelet transform domain

In the above scheme (Fig. 1) we note that there are *three* different wavelet transforms computed; one of the image $\mathcal{I}$, and one each, of the components $\frac{\partial \mathcal{I}}{\partial x}$ and $\frac{\partial \mathcal{I}}{\partial y}$ of the gradient image $\nabla \mathcal{I}$. The following question therefore suggests itself: Can the wavelet coefficients of the gradient of an image be obtained in a *simple* way from the wavelet coefficients of the image?

Since the derivative is a linear operator, its effect on the wavelet coefficients of a function of one variable is a linear transformation, characterized therefore by a matrix multiplication. Moreover, it turns out that with respect to smooth biorthogonal wavelet bases, the transform matrices are extremely simple, namely diagonal. This latter interesting observation was first made by Lemarié-Rieusset; Daubechies provides a succinct description of it in [1]. As it happens, smooth biorthogonal bases of compactly supported wavelets are ideally suited for image representation by means of wavelet coefficients, as they minimize the appearance of the distortion of edges and other transient image features incurred through image processing operations such as compression . This fortuitous coincidence enables us to obtain the wavelet coefficients of the image $\nabla \mathcal{I}$ directly, in a simple and spatially localized fashion, at each scale independently. This implies that it is necessary to compute the gradient only at desired scales; a computational advantage. For any smooth biorthogonal wavelet basis pair, there exists an associated biorthogonal wavelet basis pair, such that decomposing a function (of one variable) with respect to this associated basis and multiplying the resulting coefficient vector with a certain diagonal matrix yields the wavelet coefficients of the derivative of the function with respect to the first basis. We call this the *weak diagonalization* of the derivative operator, since different bases are used for decomposition and reconstruction.

Biorthogonal wavelet bases for representing functions of two variables (e.g., images) are obtained as scale-wise products of the above (one dimensional) biorthogonal bases in the x and y variables. Thus, associated partial derivative bases of a standard two-dimensional biorthogonal basis can be obtained by taking mixed scale-wise products of a basis in one variable and its associated derivative basis, in the other variable. As there are two such possible product bases, one for $\frac{\partial}{\partial x}$, and one for $\frac{\partial}{\partial y}$, we have a pair of associated *hybrid* biorthogonal basis pairs. Decomposing an image via a biorthogonal basis and applying certain almost-diagonal linear transformations on the resulting image wavelet coefficients, yields the wavelet coefficients of the partial derivatives of the image with respect to the associated hybrid biorthogonal bases. Figure 3 illustrates the almost-diagonal transformation matrices that represent the operator $\frac{\partial}{\partial x}$ at scale j, acting on the subband coefficients at scale j, restricted to column l, where l indexes a vertical slice of the coefficient subimages at scale j (see Appendix for details). The principal advantage of this implementation of the gradient is that, in order to compute the gradient coefficients at a particular scale, only image coefficients at that scale are used. Thus, we can acquire scale-specific image gradient information in an efficient way. This efficient implementation of the gradient in the wavelet transform domain prompts a modification of the adaptive compression schemes discussed earlier. We now briefly sketch the modified adaptive compression scheme below:

- The image $\mathcal{I}$ is decomposed in a smooth biorthogonal basis.
- The detail images are then subjected to appropriate linear transformations at desired scales to obtain the image gradient coefficients with respect to the associated hybrid (partial derivative) bases. These gradient coefficients at the desired scales are further processed to locate edge coefficients by using the edge detection scheme discussed in Appendix B.
- The edge coefficients are used to synthesize masks at desired scales, wherein the union of neighborhoods about edge coefficients is taken to form the masks .
- Image coefficients outside the neighborhoods of edge coefficients are strongly thresholded; the coefficients that fall inside the masks are either preserved or weakly thresholded.

- The resulting thresholded decomposition is then quantized and encoded to yield the adaptively compressed file.

Figure 4 illustrates the above scheme for compression.

$$
2^{-j}\begin{pmatrix}
-1 & 1 & 0 & 0 & . & . & . & 0 \\
0 & -1 & 1 & 0 & . & . & . & 0 \\
0 & 0 & -1 & 1 & . & . & . & 0 \\
. & . & . & . & . & . & . & . \\
. & . & . & . & . & . & . & . \\
0 & 0 & . & . & . & 0 & -1 & 1 \\
1 & 0 & 0 & . & . & . & 0 & -1
\end{pmatrix}
\begin{pmatrix}
h_{j;1,l} \\ h_{j;2,l} \\ h_{j;3,l} \\ . \\ . \\ h_{j;n_j-1,l} \\ h_{j;n_j,l}
\end{pmatrix}
=
\begin{pmatrix}
{}_xh_{j;1,l} \\ {}_xh_{j;2,l} \\ {}_xh_{j;3,l} \\ . \\ . \\ {}_xh_{j;n_j-1,l} \\ {}_xh_{j;n_j,l}
\end{pmatrix}
$$

$$
2^{-j}\begin{pmatrix}
4 & 0 & 0 & 0 & . & . & . & 0 \\
0 & 4 & 0 & 0 & . & . & . & 0 \\
0 & 0 & 4 & 0 & . & . & . & 0 \\
. & . & . & . & . & . & . & . \\
. & . & . & . & . & . & . & . \\
0 & 0 & . & . & . & 0 & 4 & 0 \\
0 & 0 & . & . & . & 0 & 0 & 4
\end{pmatrix}
\begin{pmatrix}
v_{j;1,l} \\ v_{j;2,l} \\ v_{j;3,l} \\ . \\ . \\ v_{j;n_j-1,l} \\ v_{j;n_j,l}
\end{pmatrix}
=
\begin{pmatrix}
{}_xv_{j;1,l} \\ {}_xv_{j;2,l} \\ {}_xv_{j;3,l} \\ . \\ . \\ {}_xv_{j;n_j-1,l} \\ {}_xv_{j;n_j,l}
\end{pmatrix}
$$

$$
2^{-j}\begin{pmatrix}
4 & 0 & 0 & 0 & . & . & . & 0 \\
0 & 4 & 0 & 0 & . & . & . & 0 \\
0 & 0 & 4 & 0 & . & . & . & 0 \\
. & . & . & . & . & . & . & . \\
. & . & . & . & . & . & . & . \\
0 & 0 & . & . & . & 0 & 4 & 0 \\
0 & 0 & . & . & . & 0 & 0 & 4
\end{pmatrix}
\begin{pmatrix}
d_{j;1,l} \\ d_{j;2,l} \\ d_{j;3,l} \\ . \\ . \\ d_{j;n_j-1,l} \\ d_{j;n_j,l}
\end{pmatrix}
=
\begin{pmatrix}
{}_xd_{j;1,l} \\ {}_xd_{j;2,l} \\ {}_xd_{j;3,l} \\ . \\ . \\ {}_xd_{j;n_j-1,l} \\ {}_xd_{j;n_j,l}
\end{pmatrix}
$$

$$
2^{-j}\begin{pmatrix}
-1 & 1 & 0 & 0 & . & . & . & 0 \\
0 & -1 & 1 & 0 & . & . & . & 0 \\
0 & 0 & -1 & 1 & . & . & . & 0 \\
. & . & . & . & . & . & . & . \\
. & . & . & . & . & . & . & . \\
0 & 0 & . & . & . & 0 & -1 & 1 \\
1 & 0 & 0 & . & . & . & 0 & -1
\end{pmatrix}
\begin{pmatrix}
s_{j;1,l} \\ s_{j;2,l} \\ s_{j;3,l} \\ . \\ . \\ s_{j;n_j-1,l} \\ s_{j;n_j,l}
\end{pmatrix}
=
\begin{pmatrix}
{}_xs_{j;1,l} \\ {}_xs_{j;2,l} \\ {}_xs_{j;3,l} \\ . \\ . \\ {}_xs_{j;n_j-1,l} \\ {}_xs_{j;n_j,l}
\end{pmatrix}
$$

Fig. 3: The four transformation matrices at scale j. The l^{th} column coefficients $\{h_{j;k,l}\}_{k=1}^{n_j}$, $\{v_{j;k,l}\}_{k=1}^{n_j}$, $\{d_{j;k,l}\}_{k=1}^{n_j}$ and $\{s_{j;k,l}\}_{k=1}^{n_j}$, belong to the horizontal, vertical, diagonal and average (low-pass) subbands at scale j, respectively, of the wavelet transform of $\mathcal{I}$, while $\{{}_xh_{j;k,l}\}_{k=1}^{n_j}$, $\{{}_xv_{j;k,l}\}_{k=1}^{n_j}$, $\{{}_xd_{j;k,l}\}_{k=1}^{n_j}$ and $\{{}_xs_{j;k,l}\}_{k=1}^{n_j}$ are the corresponding coefficients of $\frac{\partial\mathcal{I}}{\partial x}$. Similar relations hold for $\frac{\partial\mathcal{I}}{\partial y}$, with the horizontal and vertical subband matrices interchanged, and subband coefficient rows transformed instead of subband coefficient columns.

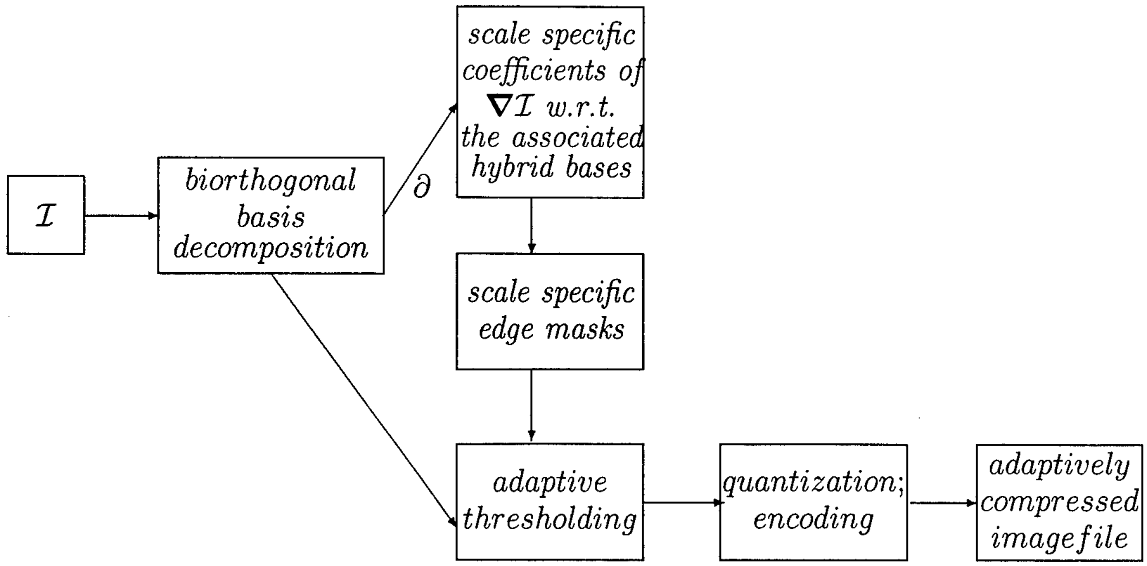

Fig.4: Schematic diagram of the modified adaptive compression scheme, using a smooth, compactly supported biorthogonal wavelet decomposition of the image $\mathcal{I}$. ∂ is the set of almost-diagonal linear transformations in Fig. 3 , applied at selected scales to compute the gradient wavelet coefficients.

A Appendix: The gradient operator in the wavelet transform domain

A.1 Preliminaries

An image $I = (I(i,j))_{i,j=0}^{N-1}$ is the discrete sampling of a compactly supported function $I(x,y)$ of $L^2(\mathbb{R}^2)$.

If $\{V_n\}_{-\infty}^{\infty}$ is a multiresolution analysis (MRA) of $L^2(\mathbb{R})$,with scaling function ϕ and wavelet ψ, then it induces an MRA of $L^2(\mathbb{R}^2)$:

$$\{\mathbf{V}_n = V_n \otimes V_n\}_{n=-\infty}^{\infty}.$$

The subspaces $\mathbf{V}_j, j \in \mathbf{Z}$ are spanned by the set of functions

$$\left\{\Phi_{j;k,l}(x,y) = 2^{-j}\Phi(2^{-j}x - k, 2^{-j}y - l) = 2^{-j}\phi(2^{-j}x - k)\phi(2^{-j}y - l)\right\}_{k,l=-\infty}^{\infty}$$

The corresponding wavelet basis of $L^2(\mathbb{R}^2)$ is given by:

$$\left\{\left\{\Psi_{j;k,l}^{\mathbf{H}}(x,y), \Psi_{j;k,l}^{\mathbf{V}}(x,y), \Psi_{j;k,l}^{\mathbf{D}}(x,y)\right\}_{k,l=-\infty}^{\infty}\right\}_{j=-\infty}^{\infty},$$

where

$$\Psi_{j;k,l}^{\mathbf{H}}(x,y) = 2^{-j}\phi(2^{-j}x - k)\psi(2^{-j}y - l)$$

$$\Psi^{\mathbf{V}}_{j;k,l}(x,y) = 2^{-j}\psi(2^{-j}x-k)\phi(2^{-j}y-l)$$

and

$$\Psi^{\mathbf{D}}_{j;k,l}(x,y) = 2^{-j}\psi(2^{-j}x-k)\psi(2^{-j}y-l).$$

If $\mathcal{I}(x,y)$ is the projection of $I(x,y)$ onto the subspace $\mathbf{V}_0$, then

$$\mathcal{I}(x,y) = \sum_{k,l=0}^{N-1} s_{0;k,l}\Phi_{0;k,l}(x,y)$$

A finite scale wavelet decomposition of $\mathcal{I}$ is then given by

$$\mathcal{I}(x,y) = \sum_{j=1}^{J}\sum_{k,l=0}^{\frac{N}{2^{-j}}-1}\left[h_{j;k,l}\Psi^{\mathbf{H}}_{j;k,l}(x,y) + v_{j;k,l}\Psi^{\mathbf{V}}_{j;k,l}(x,y) + d_{j;k,l}\Psi^{\mathbf{D}}_{j;k,l}(x,y)\right] + \sum_{k,l=0}^{\frac{N}{2^{-J}}-1} s_{J;k,l}\Phi_{J;k,l}(x,y)$$

This corresponds to a pyramidal decomposition of the image $\mathcal{I}$

$$\mathcal{I} \mapsto \left\{\left\{\left(\mathcal{I}^{\mathbf{H}}_j, \mathcal{I}^{\mathbf{V}}_j, \mathcal{I}^{\mathbf{D}}_j\right)\right\}_{j=1}^{J}, \mathcal{I}^{\mathbf{L}}_J\right\},$$

where

$$\mathcal{I}^{\mathbf{H}}_j = \left(d^{\mathbf{H}}_{j;k,l}\right)_{0\le k,l\le \frac{N}{2^j}} \mathcal{I}^{\mathbf{V}}_j = \left(d^{\mathbf{V}}_{j;k,l}\right)_{0\le k,l\le \frac{N}{2^j}} \mathcal{I}^{\mathbf{D}}_j = \left(d^{\mathbf{D}}_{j;k,l}\right)_{0\le k,l\le \frac{N}{2^j}} \quad \forall\, 1\le j\le J$$

are the high-pass (detail) subimages at resolution level j with horizontal, vertical and diagonal directionalities, respectively, and $\mathcal{I}^{\mathbf{L}}_J$ is a low-pass (average) subimage at resolution level J.

For images, it is more appropriate to use *biorthogonal* wavelets for decomposition and reconstruction, as such wavelets allow both symmetry (antisymmetry) and compactness of support; these are important properties for images, since they minimize image distortion and localize wavelet coefficients, respectively.

If $f \in L^2(\mathbb{R})$ and $\left\{\psi, \tilde{\psi}\right\}$ is a biorthogonal pair of wavelets in $L^2(\mathbb{R})$, then they generate a pair of *dual* bases of $L^2(\mathbb{R})$: $\{\psi_{j,k}\}_{j,k\in\mathbf{Z}}$ and $\left\{\tilde{\psi}_{j,k}\right\}_{j,k\in\mathbf{Z}}$, with the properties

$$f = \sum_{j,k\in\mathbf{Z}} \langle f, \psi_{j,k}\rangle \tilde{\psi}_{j,k} = \sum_{j,k\in\mathbf{Z}} \langle f, \tilde{\psi}_{j,k}\rangle \psi_{j,k}$$

and

$$\langle \psi_{j,k}, \tilde{\psi}_{j',k'}\rangle = \delta_{j,j'}\delta_{k,k'}.$$

A.2 Derivative biorthogonal wavelet bases

If $\left\{\{\psi_{j,k}\}_{j,k\in\mathbf{Z}}, \left\{\tilde{\psi}_{j,k}\right\}_{j,k\in\mathbf{Z}}\right\}$ is a compactly supported symmetric/antisymmetric biorthogonal pair of wavelet bases,then there exists (see [1]) an associated pair of *derivative* biorthogonal bases: $\left\{\left\{\psi^{\sharp}_{j,k}\right\}_{j,k\in\mathbf{Z}}, \left\{\tilde{\psi}^{\sharp}_{j,k}\right\}_{j,k\in\mathbf{Z}}\right\}$, that are also compactly supported and antisymmetric/symmetric and satisfy

$$(\psi_{j,k})' = 2^{-j+2}\psi^{\sharp}_{j,k}$$

i.e.,

$$\langle\frac{d}{dx}\psi_{j,k}, \tilde{\psi}^{\sharp}_{j',k'}\rangle = 2^{-j+2}\delta_{j,j'}\delta_{k,k'}.$$

In other words, with respect to the above two pairs of biorthogonal bases the derivative operator is diagonal.This is termed weak-diagonalization.

The scaling functions of the two basis pairs bear the following relation

$$(\phi_{j,k})' = 2^{-j}\left(\phi^{\sharp}_{j,k-1} - \phi^{\sharp}_{j,k}\right).$$

Thus if $f \in L^2(\mathbb{R})$, then

$$\langle f', \psi_{j,k}\rangle = -2^{-j+2}\langle f, \psi^{\sharp}_{j,k}\rangle,$$

and

$$\langle f', \phi_{j,k}\rangle = 2^{-j}\left(\langle f, \phi^{\sharp}_{j,k}\rangle - \langle f, \phi^{\sharp}_{j,k-1}\rangle\right).$$

A.3 Weak-diagonal representation of the image gradient

From the wavelet coefficients of an image with respect to a standard biorthogonal basis, it is possible to obtain wavelet coefficients of the gradient of the image with respect to certain associated *hybrid* derivative biorthogonal bases,

The gradient of the image $\mathcal{I}(x,y)$,denoted $\nabla\mathcal{I}(x,y)$ is the vector image given by $\nabla\mathcal{I} = \left(\frac{\partial\mathcal{I}}{\partial x}, \frac{\partial\mathcal{I}}{\partial y}\right)$.

We can write

$$\begin{aligned}
\mathcal{I}(x,y) &= \sum_{j=1}^{J}\sum_{k,l=0}^{\frac{N}{2^{-j}}-1}\left[h_{j;k,l}\Psi^{\mathbf{H}}_{j;k,l}(x,y) + v_{j;k,l}\Psi^{\mathbf{V}}_{j;k,l}(x,y) + d_{j;k,l}\Psi^{\mathbf{D}}_{j;k,l}(x,y)\right] \\
&\quad + \sum_{k,l=0}^{\frac{N}{2^{-J}}-1} s_{J;k,l}\Phi_{J;k,l}(x,y) \\
&= \sum_{j;k,l}\left[h_{j;k,l}\phi_{j;k}(x)\psi_{j;l}(y) + v_{j;k,l}\psi_{j;k}(x)\phi_{j;l}(y) + d_{j;k,l}\psi_{j;k}(x)\psi_{j;l}(y)\right] \\
&\quad + \sum_{k,l} s_{J;k,l}\phi_{J;k}(x)\phi_{J;l}(y)
\end{aligned}$$

where

$$h_{j;k,l} = \langle \mathcal{I}, \tilde{\Psi}^{\mathbf{H}}_{j;k,l} \rangle = \langle \mathcal{I}, \tilde{\phi}_{j;k}\tilde{\psi}_{j;l} \rangle$$
$$v_{j;k,l} = \langle \mathcal{I}, \tilde{\Psi}^{\mathbf{V}}_{j;k,l} \rangle = \langle \mathcal{I}, \tilde{\psi}_{j;k}\tilde{\phi}_{j;l} \rangle$$
$$d_{j;k,l} = \langle \mathcal{I}, \tilde{\Psi}^{\mathbf{D}}_{j;k,l} \rangle = \langle \mathcal{I}, \tilde{\psi}_{j;k}\tilde{\psi}_{j;l} \rangle$$

and

$$s_{J;k,l} = \langle \mathcal{I}, \tilde{\Phi}_{J;k,l} \rangle = \langle \mathcal{I}, \tilde{\phi}_{J;k}\tilde{\phi}_{J;l} \rangle$$

are the wavelet and scaling function coefficients w.r.t. the dual basis.

Then

$$\begin{aligned}
\frac{\partial \mathcal{I}}{\partial x} &= \sum_{j;k,l} \Big[h_{j;k,l} \left(\phi_{j;k}(x)\right)' \psi_{j;l}(y) + v_{j;k,l} \left(\psi_{j;k}(x)\right)' \phi_{j;l}(y) + d_{j;k,l} \left(\psi_{j;k}(x)\right)' \psi_{j;l}(y) \Big] \\
&\quad + \sum_{k,l} s_{J;k,l} \left(\phi_{J;k}(x)\right)' \phi_{J;l}(y) \\
&= \sum_{j;k,l} \Big[{}_x h_{j;k,l} \phi^{\sharp}_{j;k}(x) \psi_{j;l}(y) + {}_x v_{j;k,l} \psi^{\sharp}_{j;k}(x) \phi_{j;l}(y) + {}_x d_{j;k,l} \psi^{\sharp}_{j;k}(x) \psi_{j;l}(y) \Big] \\
&\quad + \sum_{k,l} {}_x s_{J;k,l} \phi^{\sharp}_{J;k}(x) \phi_{J;l}(y) \\
&= \sum_{j=1}^{J} \sum_{k,l=0}^{\frac{N}{2^{-j}}-1} \Big[{}_x h_{j;k,l}\, {}_x\Psi^{\mathbf{H}}_{j;k,l}(x,y) + {}_x v_{j;k,l}\, {}_x\Psi^{\mathbf{V}}_{j;k,l}(x,y) + {}_x d_{j;k,l}\, {}_x\Psi^{\mathbf{D}}_{j;k,l}(x,y) \Big] \\
&\quad + \sum_{k,l=0}^{\frac{N}{2^{-J}}-1} {}_x s_{J;k,l}\, {}_x\Phi_{J;k,l}(x,y)
\end{aligned}$$

where

$$\left.\begin{aligned}
{}_x h_{j;k,l} &= 2^{-j} \left(h_{j;k+1,l} - h_{j;k,l} \right) \\
{}_x v_{j;k,l} &= 2^{-j+2} v_{j;k,l} \\
{}_x d_{j;k,l} &= 2^{-j+2} d_{j;k,l} \\
{}_x s_{j;k,l} &= 2^{-j} \left(s_{j;k+1,l} - s_{j;k,l} \right)
\end{aligned}\right\} = \partial^j_x$$

are scale-space-subband localized, almost-diagonal linear transformations on the wavelet and scaling function coefficients of the wavelet transform of $\mathcal{I}$, w.r.t. the biorthogonal basis $\mathcal{B} = \left\{ \Psi^{\mathbf{H}}_{j;k,l}, \Psi^{\mathbf{V}}_{j;k,l}, \Psi^{\mathbf{D}}_{j;k,l} \right\}_{j,k,l \in \mathbf{Z}}$. These transformations yield the wavelet and scaling function coefficients of the wavelet transform of $\frac{\partial \mathcal{I}}{\partial x}$, w.r.t. the associated x-derivative biorthogonal basis ${}_x\mathcal{B} = \left\{ {}_x\Psi^{\mathbf{H}}_{j;k,l}, {}_x\Psi^{\mathbf{V}}_{j;k,l}, {}_x\Psi^{\mathbf{D}}_{j;k,l} \right\}_{j,k,l \in \mathbf{Z}}$.

Similarly,

$$\begin{aligned}
\frac{\partial \mathcal{I}}{\partial y} &= \sum_{j;k,l}\left[h_{j;k,l}\phi_{j;k}(x)\left(\psi_{j;l}(y)\right)' + v_{j;k,l}\psi_{j;k}(x)\left(\phi_{j;l}(y)\right)' + d_{j;k,l}\psi_{j;k}(x)\left(\psi_{j;l}(y)\right)'\right] \\
&\quad + \sum_{k,l} s_{J;k,l}\phi_{J;k}(x)\left(\phi_{J;l}(y)\right)' \\
&= \sum_{j;k,l}\left[{}_y h_{j;k,l}\phi^{\sharp}_{j;k}(x)\psi_{j;l}(y) + {}_y v_{j;k,l}\psi^{\sharp}_{j;k}(x)\phi_{j;l}(y) + {}_y d_{j;k,l}\psi^{\sharp}_{j;k}(x)\psi_{j;l}(y)\right] \\
&\quad + \sum_{k,l} {}_y s_{J;k,l}\phi^{\sharp}_{J;k}(x)\phi_{J;l}(y) \\
&= \sum_{j=1}^{J}\sum_{k,l=0}^{\frac{N}{2^{-j}}-1}\left[{}_y h_{j;k,l}\,{}_y\Psi^{\mathbf{H}}_{j;k,l}(x,y) + {}_y v_{j;k,l}\,{}_y\Psi^{\mathbf{V}}_{j;k,l}(x,y) + {}_y d_{j;k,l}\,{}_y\Psi^{\mathbf{D}}_{j;k,l}(x,y)\right] \\
&\quad + \sum_{k,l=0}^{\frac{N}{2^{-J}}-1} {}_y s_{J;k,l}\,{}_y\Phi_{J;k,l}(x,y)
\end{aligned}$$

where

$$\left.\begin{aligned}
{}_y h_{j;k,l} &= 2^{-j+2}h_{j;k,l} \\
{}_y v_{j;k,l} &= 2^{-j}\left(v_{j;k,l+1} - v_{j;k,l}\right) \\
{}_y d_{j;k,l} &= 2^{-j+2}d_{j;k,l} \\
{}_y s_{j;k,l} &= 2^{-j}\left(s_{j;k,l+1} - s_{j;k,l}\right)
\end{aligned}\right\} = \partial^j_y$$

are scale-space-subband localized, almost-diagonal linear transformations on the wavelet and scaling function coefficients of the wavelet transform of $\mathcal{I}$, w.r.t. the biorthogonal basis $\mathcal{B} = \left\{\Psi^{\mathbf{H}}_{j;k,l}, \Psi^{\mathbf{V}}_{j;k,l}, \Psi^{\mathbf{D}}_{j;k,l}\right\}_{j,k,l\in\mathbf{Z}}$. These transformations yield the wavelet and scaling function coefficients of the wavelet transform of $\frac{\partial \mathcal{I}}{\partial y}$, w.r.t. the associated y-derivative biorthogonal basis ${}_y\mathcal{B} = \left\{{}_y\Psi^{\mathbf{H}}_{j;k,l}, {}_y\Psi^{\mathbf{V}}_{j;k,l}, {}_y\Psi^{\mathbf{D}}_{j;k,l}\right\}_{j,k,l\in\mathbf{Z}}$.

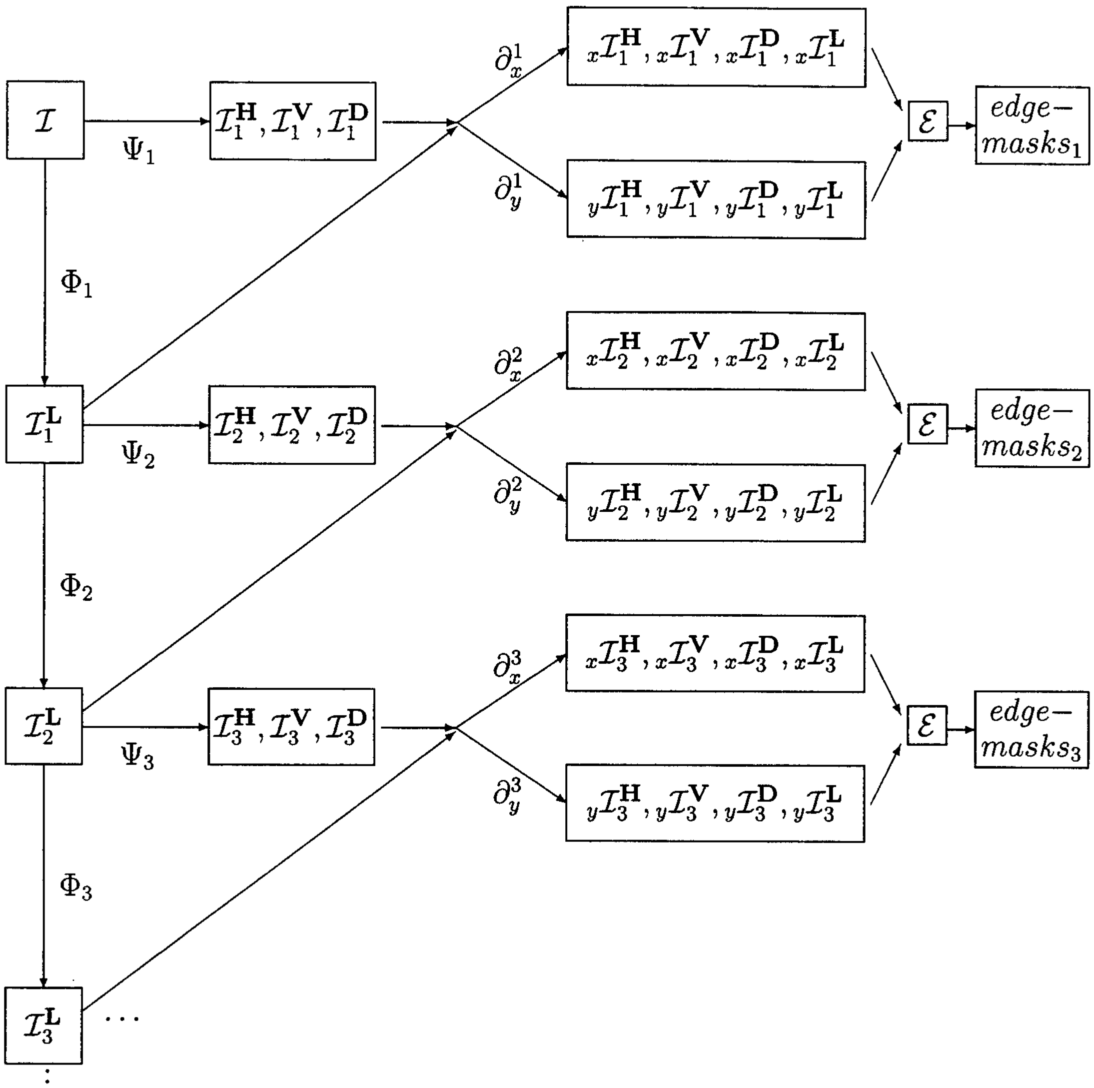

Fig 5: coefficient location scheme for three levels of scale used in adaptive compression of images.
Ψ_j and Φ_j are the detail and average filtering operations at scale j. $\mathcal{I}_j^{\mathbf{H}}, \mathcal{I}_j^{\mathbf{V}}, \mathcal{I}_j^{\mathbf{D}}$ and $\mathcal{I}_j^{\mathbf{L}}$ are the horizontal, vertical, diagonal detail subimages and average (low-pass) subimage, respectively, at scale j.
∂_x^j and ∂_y^j are the linear transformations performed on subimage coefficients at scale j, to obtain the gradient subimage coefficients ${}_x\mathcal{I}_j^{\mathbf{H}}$, ${}_x\mathcal{I}_j^{\mathbf{V}}$, ${}_x\mathcal{I}_j^{\mathbf{D}}$, ${}_x\mathcal{I}_j^{\mathbf{L}}$ and ${}_y\mathcal{I}_j^{\mathbf{H}}$, ${}_y\mathcal{I}_j^{\mathbf{V}}$, ${}_y\mathcal{I}_j^{\mathbf{D}}$, ${}_y\mathcal{I}_j^{\mathbf{L}}$, w.r.t. the associated derivative biorthogonal bases.
$\mathcal{E}$ is a process that extracts the edge coefficients of the gradient subimages, and *edgemasks*$_j$ are the mask templates at scale j. The positions and scales of the edge coefficients of the gradient image and those of the image coincide.

B Appendix: Edge Coefficient Detection

The edge pixels in an image correspond to the modulus maxima (i.e., the maxima of $\nabla\mathcal{I}\cdot\nabla\mathcal{I}$) of the gradient of the image. However, not every modulus maximum of the gradient image is the result of an edge pixel in the original image; certain textures can also give rise to modulus maxima. There are certain necessary conditions that a pixel p corresponding to a modulus maximum of the gradient of an image must satisfy, in order to qualify as an edge pixel. We enumerate them below:

i) There must exist at least one neighboring (adjacent) pixel that is also a modulus maximum of the image gradient. This is because edges are contiguous objects, and do not occur as isolated pixels.

ii) There must exist at least one pixel satisfying condition i), at which the magnitude of the modulus maximum is close to that at the pixel p. This is because the strength of an edge varies slowly along the edge.

iii) There must exist at least one pixel satisfying condition ii), such that the line joining this pixel to the pixel p is close to being perpendicular to the direction of the gradient at p. This is because the gradient vector at an edge point is perpendicular to the local orientation of the edge at that point.

The satisfaction of the above criteria by a gradient modulus maximum pixel is not sufficient to qualify it as an edge pixel. Textures in an image may possess edge feature elements (as in a reticulation, for instance,) that may not be the *desired* edges of the image. By demanding, that, edges must have a certain minimum length, and that the average grey value on any given side of an edge remain constant, one may be able to eliminate candidate edge pixels that are not part of "genuine" edges of the image. Such conditions that help prune the set of candidate edge pixels, are largely heuristic, and vary with the nature and characteristics of the image that is being analysed. One can however construct rules using which it is possible to filter edge features , so as to retain only desired edges. We, however, would like to identify edge coefficients in the transform domain of the image, and not edge pixels. The above conditions and constraints can be ported to the transform domain as well.

At any scale j, the image gradient's modulus at any position is estimated by summing the absolute values of all the subband coefficients corresponding to that position. From this we can obtain the positions of the modulus maxima of the gradient at scale j. Condition i) translates to eliminating coefficients that correspond to isolated maxima at scale j. Condition ii) carries over unchanged to the case of coefficients (instead of pixels) at scale j. These two conditions isolate from the set of all coefficients corresponding to modulus maxima of the gradient coefficients at scale j, a subset consisting of coefficients forming maxima chains of two or more coefficients. We can now invert the coefficients of these maxima chains to obtain the components of the gradient vectors at the positions of the coefficients in the maxima chains at scale j. This operation of obtaining the gradient vectors is computationally very efficient, since, a) in general, the maxima chain set is a tenuous subset of the coefficient set at scale j, b) the inverse transform is a local operation, c) this inversion is performed at only desired scales.

Having obtained the gradient vector (and hence its direction) at each of the coefficient locations corresponding to coefficients of the maxima chain set, we can then proceed to apply condition iii) to the coefficients at scale j.

Certain rules and constraints that are not easy to formulate in the image domain may be possible to impose in the transform domain; such as, demanding that the neighborhood of an edge coefficient at a given scale must correspond to (e.g., overlap with,) edge coefficient neighborhoods at certain other scales. Each chain component of edge coefficients obtained by the above scheme is augmented by adding to it the 3×3-neighborhoods (of coefficients) of each of its edge coefficients, thus generating an edge mask at that scale for that edge. This entire procedure of edge coefficient detection and generation of edge masks at each scale is schematically illustrated by the procedure denoted $\mathcal{E}$ in Fig. 5 .

References

[1] I.C. Daubechies. Two recent results on wavelets. in *Recent Advances in Wavelet Analysis.* L.L. Schumaker and G. Webb Eds. Academic Press, San Diego, CA, 1994. pp 251-257.

[2] I.C. Daubechies. *Ten Lectures on Wavelets.* SIAM, Philadelphia, PA, 1992.

[3] A. Cohen, I.C. Daubechies and J-C Feauveau. Biorthogonal bases of compactly supported wavelets. *Comm. Pure and Appl. Math.*, Vol 45, 1992. pp 485-560.

[4] J. Froment and S. Mallat. Second generation compact image coding with wavelets. in *WAVELETS: A Tutorial in Theory and Applications.* C.K. Chui Ed. Academic Press, San Diego, CA, 1992. pp 655-677.

[5] S. Carlsson. Sketch based coding of grey level images. *Signal Processing* **15**. 1988 pp 57-83.

[6] J. Canny. A Computational approach to edge detection. *IEEE Trans. on Patt. Anal. and Mach. Intel.* Vol. PAMI-8, No. 6. Nov. 1986. pp 679-698.p

[7] G. Zweig. Image Processing with wavelet coefficients. *A research proposal in response to BAA 95-1 of NRL (Remote Sensing, code 7240).* Aug. 1995.